SPECTRALLY DEFINED COMPOSITION OF THE CONNECTING RIDGE BETWEEN SHACKLETON AND HENSON CRATERS IN PREPARATION FOR ARTEMIS EXTRA VEHICULAR ACTIVITIES. M. Lemelin[1], D. A. Kring[2], C. van der Bogert[3], H. Hiesinger[3], L. Gaddis[2], G. R. Osinski[4] [1]Département de Géomatique appliquée, Université de Sherbrooke, Qc, Canada, J1K 2R1 (Myriam.Lemelin@USherbrooke.ca), [2]Center for Lunar Science & Exploration, Lunar and Planetary Institute, USRA, Houston, TX 77058, [3]Institut für Planetologie, Westfälische Wilhelms-Universität, 48149 Münster, Germany, [4]Dept. Earth Sciences/Institute for Earth and Space Exploration, University of Western Ontario, London, Canada.

Introduction: The Artemis III mission will be the first human mission to the lunar surface in the 21st century. Building upon the legacy of the Apollo era, the goal is to develop sustainable human exploration of the Moon and deep space. Seven science objectives have been defined by the NASA Science Mission Direcorate for Artemis III [1]: (1) Understanding planetary processes, (2) Understanding the character and origin of lunar polar volatiles, (3) Interpreting the impact history of the Earth-Moon system, (4) Revealing the record of the ancient Sun and our astronominal environment, (5) Observing the universe and the local space environment from a unique location, (6) Conducting experimental science in the lunar environment, and (7) Investigating and mitigating exploration risks. Currently, Human Landing System capabilities are being refined while mission architectural details and potential landing sites are being evaluated. In parallel, future activities related to field geology, sample collection and return, *in situ* and field science, and deployable experiments are being investigated to form a cohesive program [1].

Artemis III is targeting a landing site in the south polar region of the Moon, between 84 and 90°S. The precise landing site has not yet been determined, but six regions of interest have been identified (sites 001, 004, 007, 011, 102 and 105, [1]; Fig. 1). These sites occur in some of the most illuminated south polar regions [2] and are located near permanently shadowed regions (PSRs) that may contain volatiles. These regions may provide long-duration access to sunlight, direct-to-Earth communication, as well as surface slopes and roughness favorable for landers and astronauts [1].

Here we characterize the surface composition surrounding sites 001 (89.45ºS, 137.37ºW) and 004 (89.78ºS, 155.73ºW) in preparation for future Artemis activities related to field geology, sample collection and return, and *in situ* and field science, which will help define which of the seven Artemis objectives can be addressed. To do so, we use polar mineral maps derived from the Kaguya Spectral Profiler and Lunar Orbiter Laser Altimeter (LOLA) data of [3,4] as well as individual Kaguya Spectral Profiler spectra [5,6].

Data and methods: The Kaguya Spectral Profiler is a point spectrometer which conducted continuous spectral observations of the lunar surface in the VIS/NIR region (500 to 2600 nm) between years 2007 and 2009, with a spatial resolution of ~500 m/pixel [5,6]. Spectral Profiler data level 2B1 contains radiometrically calibrated radiance data that can be converted to diffuse reflectance using a photometric function that normalizes the reflectance (at an incidence angle of 30° and emission angle of 0°). Lemelin et al. [3,4] filtered tens of millions of Spectral Profiler spectra and used those that have an acceptable signal-to-noise ratio and radiance value (~9 million in each polar region) to convert them into reflectance, grid the values at 1 km/pixel, and interpolate missing values. However, as photometric functions assume a flat sphere, important reflectance artifacts are observed in the polar regions on slopes. To remove this effect, they normalized gridded Spectral Profiler data to the gridded and calibrated 1 km/pixel LOLA dataset [7]. Lemelin et al. [3,4] then used the gridded and calibrated Spectral Profiler dataset to quantify the abundance of FeO, minerals (olivine, pyroxenes and plagioclase), nanophase iron and optical maturity (OMAT) at 1 km/pixel in both polar regions. Here we use these recent maps (1 km/pixel) as well as individual Spectral Profiler spectra (~500 m/pixel) to characterize the composition surrounding sites 001 and 004.

Results: The compositional maps produced by [3,4] suggest that the initial Artemis exploration region (84 to 90°S) is characterized by relatively homogeneous FeO (~5 to 10 wt%; Fig. 1) and plagioclase (~70 to 90 wt%) content at the observed spatial resolution of 1 km/pixel.

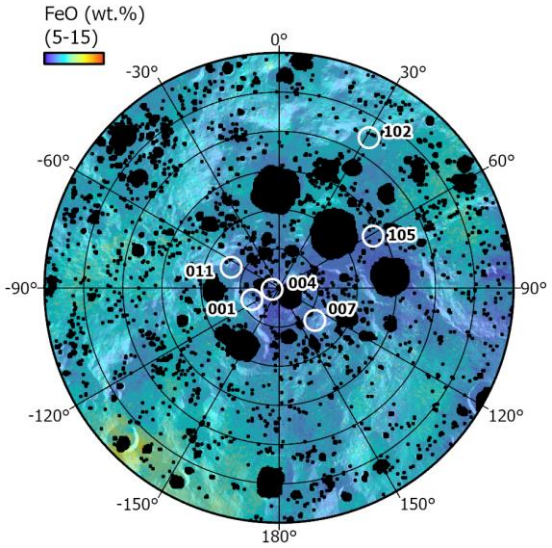

Figure 1. FeO content within the Artemis region (84 to 90°S) mapped by Lemelin et al. [3,4]. White circles represent potential Artemis III sites, black polygons PSRs (taken from [4]).

The lowest gridded FeO values (~5 to 7 wt.%) are found in the 89 to 90°S region around Shackleton crater (including sites 001 and 004), between Shoemaker and Faustini craters as well as on the central peak of Amundsen. These regions also correspond to regions with the highest plagioclase content (~80 to 90 wt%, Fig. 2), representative of noritic/gabbroic or troctolitic anorthosite. The gridded maps do not reveal the presence of anorthosites (>90 wt.% plagioclase), such as the exposures of pure anorthosite (≥98 wt.% plagioclase) detected on the upper crater walls of Shackleton crater by [8,9]. We hypothesize that these exposures are not apparent in the gridded maps as the gridding process lowered the spatial resolution of the original data and averaged the spectral signatures of nearby data points, which could include mixtures of anorthosites and more mafic ejecta from the South Pole Aitken basin. We searched through the Spectral Profiler (ungridded and unnormalized) data to localize potential exposures of anorthosite (>90 wt.% plagioclase) as those having a high signal (radiance value at 753 nm >23 $w/m^{-2}/um^{-1}/sr^{-1}$) and a 1.25 µm absorption band consistent with the presence of anorthosite (continuum removed reflectance minimum between 1.20 and 1.35 µm) [8,10]. Many such exposures are likely present on the wall of Shackleton and some on the connecting ridge between Shackleton and Henson (Fig. 2).

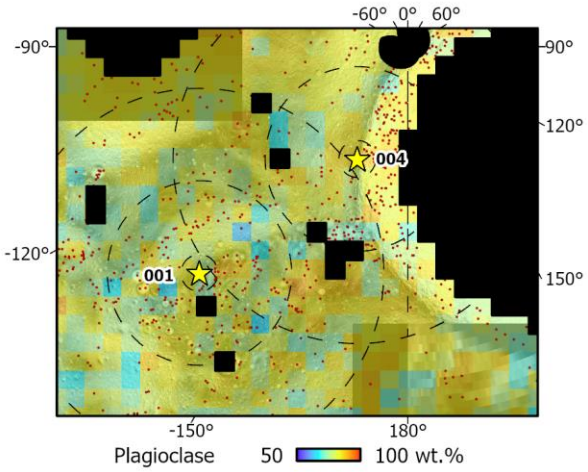

Figure 2. Plagioclase content and potential exposures of anorthosites (red points) in the Artemis 001-004 region. Black polygons represent PSRs, dashed lines 1, 5 and 10 km buffers around sites 001 and 004.

The south polar OMAT map [4] suggests that the entire Artemis region is characterized by high OMAT values (low optical maturity) (Fig. 3). However, the potential contribution of at least two craters seem to locally enhance these values: Tycho and De Forest. It appears that rays coming from Tycho may extend to the south pole, likely in the region surrounding sites 001-004.

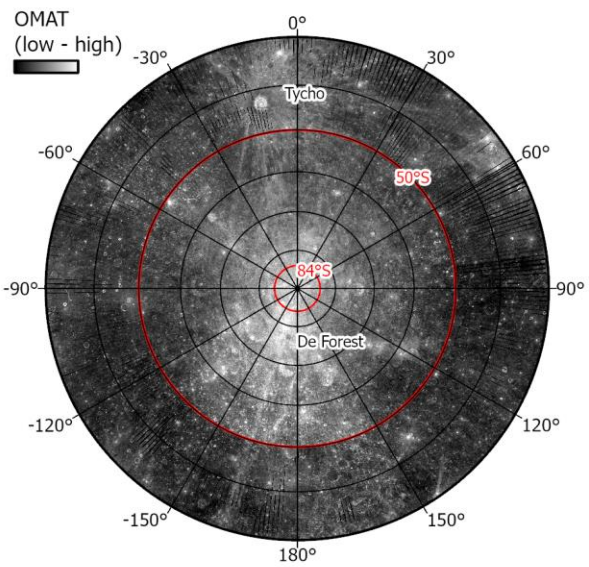

Figure 3. Optical maturity (OMAT) map of the south polar region (30-90°S). Bright OMAT rays extend from Tycho and De Forest craters into the Artemis region (taken from [4]).

Conclusion: The mineral maps derived by [4] offer the first compositional view of the Artemis region. The region surrounding sites 001-004 seems to be particularly appealing for its geology (low FeO content, presence of anorthosite and ejecta from young and distant craters) which would help in understanding planetary processes as well as the impact history of the Earth-Moon system. A companion abstract [11] focusing on the detection of volatiles in the polar regions suggests that this region might also help in understanding the character and origin of lunar polar volatiles.

In the near future, considerable efforts should be taken to derive compositional maps of the Artemis region at a higher spatial resolution. Data acquired by the Imaging Infrared Spectrometer (IIRS, 80 m/pixel) onboard the Chandrayaan-2 might offer this opportunity soon, but the data currently released is restricted to 0 to 30ºN/S. Data acquired by the High-resolution Volatiles and Minerals Moon Mapper (HVM^3) onboard Lunar Trailblazer will not be available until ~2025.

References: [1] NASA (2020) Artemis III SDT report. [2] Mazarico et al. (2011) *Icarus, 211*,1066-1081. [3] Lemelin et al. (2021) *LPSC 52, #1038*. [4] Lemelin et al. (2022) *PSJ, accepted*. [5] Matsunaga T. et al. (2001) *Proc. SPIE*, *4151*, 32-39. [6] Haruyama J. et al. (2008) *EPS, 60*, 243-255. [7] Lemelin M. et al. (2016) *Icarus, 273*, 315-328. [8] Yamamoto et al. (2012), *GRL, 39*, L13201. [9] Lemelin et al. (2017) *LPSC 48, #2479*. [10] Cheek et al. (2013) *JGR, 118*, 1805-1820. [11] Lemelin et al. (2022) *LPSC 53, #1700*.